2014년도 2월
석사학위논문

# Effects of histone deacetylase inhibitors on epigenetic modification in human bone marrow mesenchymal stem cells

조 선 대 학 교 대 학 원

생 명 과 학 과

정 신 구

# Effects of histone deacetylase inhibitors on epigenetic modification in human bone marrow mesenchymal stem cells

인간 유래 골수 줄기세포에서 후생유전체 변형에 관한 히스톤 탈아세틸화 억제제의 영향

2014 년 2 월 25 일

조 선 대 학 교 대 학 원

생 명 과 학 과

정 신 구

# Effects of histone deacetylase inhibitors on epigenetic modification in human bone marrow mesenchymal stem cells

지도교수 조광원

이 논문을 이학석사학위 신청 논문으로 제출함

2013 년 10월

조 선 대 학 교 대 학 원

생 명 과 학 과

정 신 구

# 정신구의 석사학위논문을 인준함

위원장 조선대학교 부교수 박 현 용 (인)

위 원 조선대학교 조교수 전 택 중 (인)

위 원 조선대학교 조교수 조 광 원 (인)

2013년 11월

조선대학교 대학원

# CONTENTS

Part II

# List of Figures

## Part I



## Part II

# List of Table

## Part I

## Abbreviations

| | |
|---|---|
| BHA | Butylated hydroxyanisole |
| BM-MSCs | Bone marrow-mesenchymal stromal cells |
| CNS | Central nervous system |
| FBS | Fetal bovine serum |
| HDAC | Histone deacetylase |
| HSC | Hematopoietic stem cells |
| MSCs | Mesenchymal stromal cells |
| PBS | Phosphate-buffered saline |
| PCR | Polymerase chain reaction |
| ROS | Reactive oxygen species |
| RT | Room temperature |
| VPA | Valproic acid |
| ROS | Reactive oxygen species |
| TSA | Trichostatin A |
| SA | Sodium arsenite |
| DCFH-DA | 2'-7'-Dichlorodihydrofluorescein diacetate |

# Abstract

## Effects of histone deacetylase inhibitors on epigenetic modification in human bone marrow mesenchymal stem cells

Sin-Gu Jeong

Advisor : Assistant Prof. Goang-Won Cho, Ph.D.

Department of life science,

Graduate school of Chosun University

Somatic stem cells can provide properly differentiated cells to restore the function of tissues in the human body damaged by several factors, including reactive oxygen species (ROS) production and inflammation. As unhealthy or older people often fail to replace their damaged cells due to functional weakness at their stem cells, stem cell therapies are an attractive option. The usage of unhealthy stem cells could give a weak therapeutic efficacy in patients; therefore, autologous stem cells need to be improved prior to applications in cell therapy. Recent studies have shown that inhibition of histone deacetylase (HDACs) have been applied in the induction of stem cell differentiation and treatment for disease. These suggest HDAC inhibitors may be good candidates for the improvement of stem cell capacities. In this study, first, I investigated the effects of a HDAC inhibitor, valproic acid (VPA), for the neuronal differentiation of human bone marrow-mesenchymal stromal cells (PART I). VPA-treated MSCs had significant increases in their

expression of the neuro-progenitor marker *Nestin*, *Musashi*, *CD133*, and *GFAP*, as measured by real-time PCR and immunoblot analysis. When VPA-pretreated MSCs were differentiated with neuronal induction media (VPA-dMSCs), they exhibited a cell body and dendritic morphology similar to neurons. The number and neurite length of these VPA-dMSCs significantly increased compared to differentiated MSCs (dMSCs). The VPA-dMSCs and dMSCs had significantly increased transcripts of neuronal-specific marker genes, including *Nestin, Musashi, CD133*, *GFAP, NeuN*, *MAP*-2, *NF-M*, *KCNH1*, *KCNH5*. The cells also showed a higher expression of the neuronal marker proteins Nestin and NF-M from immunocytochemical staining and immunoblot analysis. This study has shown that VPA pretreatment of hBM-MSCs, following their incubation with neuronal induction media, effectively stimulates neuronal cell differentiation to BM-MSCs.

Next, I investigated whether ROS are reduced by the HDAC inhibitor, trichostatin A (TSA) in human bone marrow mesenchymal stem cells (PART II). I examined the effects of TSA on ROS in hBM-MSCs through MTT assay and ROS detection. The intracellular ROS were significantly increased in hydrogen peroxide ($H_2O_2$) treated MSCs and sodium arsenite (SA) treated MSCs. When hBM-MSCs were incubated with TSA (0 ~ 5000 nM) for 8 hours, cell viability and ROS levels were not changed. The ROS induced by oxidative stress were reduced in TSA pretreated hBM-MSCs (TSA-MSCs) compared to non-treated hBM-MSCs (Stress-MSCs). In conclusion, the TSA reduced ROS in hBM-MSCs, which may protect cells from oxidative stress.

The present my studies suggest that HDAC inhibitors, TSA and VPA, effectively improves capacity of differentiation and protection. The combination of HDAC inhibitors and MSCs may improve the efficacy in the cell therapy.

# 국문초록

## 인간 유래 골수 줄기세포에서 후생유전체 변형에 관한 히스톤 탈아세틸화 억제제의 영향

성체 줄기세포는 활성산소, 염증과 같은 다양한 요인에 의한 손상된 조직의 기능을 적절한 세포로의 분화를 통해서 회복시킬 수 있다. 하지만 건강하지 못한 사람 또는 나이든 사람에서는 줄기세포의 기능적 손상으로 인해 종종 손상된 조직의 대체를 이루지 못한다. 이는 건강하지 않은 줄기세포의 이용이 환자 치료에 있어서 좋지 않은 영향을 준다는 것을 의미한다. 그러므로 줄기세포는 세포치료에 사용되기 전에 세포 자신의 기능적, 건강적 면을 향상시킬 필요가 있다. 최근 연구에서 줄기세포의 분화와 질병의 치료에 있어 히스톤 탈아세틸화 억제제가 사용된다. 이는 히스톤 탈아세틸화 억제제가 줄기세포의 능력의 향상을 시키는 우수한 물질일수 있음을 의미한다.

본 연구는 첫째로 히스톤 탈아세틸화 억제제로 알려진 발프로산의 처리를 통해 인간 유래 골수 중간엽 줄기세포의 신경세포로의 분화를 유도하는데 있어서 효과를 갖는지 연구를 진행하였다. Real-time PCR과 면역블랏을 통해 발프로산을 전처리한 중간엽 줄기세포에서 신경 전구체 마커인 *Nestin, Musashi, CD133, GFAP*의 발현이 유의성 있게 증가하는 것을 확인하였다. 발프로산 전처리와 함께 신경세포 분화 배양액을 처리하여 분화를 유도하였을 때 세포체와 수상돌기의 형태가 뉴런과 유사한 형태를 나타내었고 분화된 줄기세포와 비교하였을 때 발프로산 전처리 후 분화시킨 줄기

세포에서 분화 율과 신경돌기의 길이 또한 유의성 있게 증가하였다. 이와 함께 신경세포 특이적 표지인자인 *Nestin, Musashi, CD133, GFAP, NeuN, MAP-2, NF-M, KCNH1, KCNH5*의 발현이 분화 유도 배양액을 통해 유도된 줄기세포와 비교하였을 때 유의하게 증가함을 관찰하였다. 단백질 수준에서 관찰하였을 때 앞선 결과와 마찬가지로 발프로산 전처리를 통한 분화 세포에서 높게 발현함을 관찰하였다. 이 연구는 신경유도 배양액과 함께 발프로산을 전처리 하였을 때 인간 유래 골수 중간엽 줄기세포에서 신경세포로의 분화 효율을 높일 수 있음을 보여준다.

다음으로, 우리는 히스톤 탈아세틸화 억제제인 TSA에 의한 활성산소 조절에 관한 연구를 진행하였다. 우리는 세포생존능력 분석법과 활성산소 분석법을 통하여 줄기세포에서 활성산소에 대한 TSA의 효과를 조사하였다. 줄기세포는 과비산나트륨과 과산화수소수에 의해 활성산소가 증가함을 관찰하였고, TSA 단독 처리로 인해서는 활성산소의 변화가 없음을 관찰하였다. TSA의 전처리를 통한 줄기세포에서는 산화적 스트레스에 의해 유도된 활성산소가 TSA 전처리를 하지 않은 세포와 비교 하였을 때 유의하게 감소함을 확인하였다. 이는 TSA가 줄기세포에서 활성산소를 줄이고 이는 산화적 스트레스로부터 줄기세포의 보호 효과를 높일 수 있음을 의미한다.

이 두 가지 연구는 TSA와 발프로산의 처리를 통해 줄기세포를 이용한 세포치료법에 있어서 효율성을 증가시킬 수 있음을 의미한다.

# I. Introduction

Stem cells are functionally defined through their replicative capacity [26, 30] and ability to generate diverse differentiated cells [2, 22, 31]. Somatic stem cells can provide properly differentiated cells to restore the function of tissues in the human body damaged by several factors, including reactive oxygen species (ROS) production, inflammation, ischemia, apoptosis, and physical damage. As unhealthy or older people often fail to replace their damaged cells due to functional weakness at their stem cells [3, 5, 29], stem cell therapies are an attractive option. The usage of unhealthy stem cells could give a weak therapeutic efficacy in patients; therefore, autologous stem cells need to be improved prior to applications in cell therapy.

Histone deacetylases plays a crucial role in the suppression of diverse gene loci by altering their chromatin structure through the regulation of chromatin modulation proteins [1, 20]. Recent stem cell studies have reported that cultured hematopoietic stem cells (HSCs) are reactivated through fetal hemoglobin expression by treatment with the histone deacetylase (HDAC) inhibitor, sodium butyrate, in the presence of the c-kit ligand [8, 18, 27]. Another HDAC inhibitor, trichostatin A, has been found to promote beta-islet cell differentiation (in the presence of

glucagon) in bone marrow-mesenchymal stromal cells (BM-MSCs) [28]. Trichostatin A has also been found to stimulate myocyte growth *in vitro* and *in vivo*, and enhances myofiber size and muscle functions in dystrophic mice [13, 19]. Other studies have shown that valproic acid (VPA) induces the differentiation of hippocampus-derived neural stem cells in the central nervous system (CNS) [12, 32]. These studies suggest that HDAC inhibitors might be strong candidates for enhancing the differentiation capacities of stem cells.

Valproic acid is a short-chain fatty acid and a histone deacetylase (HDAC) inhibitor which inhibits class I and class IIa HDACs with an $IC_{50}$ in the low millimolar range [10]. This compound has been pharmacologically used for neurological diseases including epilepsy [17, 23], bipolar disorder [15], migraine headaches [25], and schizophrenia [11].

Since HDAC inhibition has been reported to induce the differentiation of stem cells [8, 12, 18, 27, 28, 32], I investigated whether VPA stimulates the neuronal differentiation of hBM-MSCs. I report here that VPA promotes neuronal differentiation by induction of neuroprogenitors in hBM-MSCs.

# II. Materials and Methods

## II-1. Characteristics of primary human BM-MSCs and cell culture

hBM-MSCs were purchased from CEFO (Cell Engineering For Origin, Korea). The cells were examined viral infection and mycoplasma contamination, presented all negative. Flow cytometric analysis of the cells revealed a $CD73^{+}$, $CD105^{+}$, $CD31^{-}$ phenotype. Real-time PCR analysis to neuronal specific markers (*musashi, nestin, CD*133*, GFAP, NeuN, NF-M*, and *KCNH5*) showed lower expression than in neuroblastoma cell SH-SY5Y while similar to those of non-neural cell HeLa (data not shown). The hBM-MSCs were cultured in T75 flasks (Becton Dickinson, USA) according to the supplier's recommendations. Cells were cultivated in hBM-MSC growth media (Gibco, USA), containing the mesenchymal cell growth supplements, L-glutamine, penicillin, and streptomycin, without any stimulatory supplements or vitamins. Cells were maintained in a humidified incubator at 37°C, using a standard mixture of 95% air and 5% $CO_2$. MSCs passaged seven times were used.

## II-2. Neuronal differentiation

hBM-MSCs were incubated with/without 200 μg/ml VPA for 12 hours

as previously described [4]. The cells were then exposed to pre-induction media containing 10% FBS, 10 ng/ml bFGF, and 500 μM β-mercaptoethanol for 24 hours. The media were replaced with induction media containing 100 μM butylated hydroxyanisole (BHA), and 2% DMSO in FBS-free media for 6 hours, according to previously described procedures [31]. Control MSCs were incubated with FBS containing media for 24 hours. The media were replaced with FBS-free media and the cells were then further incubated for 6 hours. The cell images were taken with a microscope (Olympus IX71, Japan) and a digital camera (Olympus U-LS30-3, Japan). Neurite lengths were measured using the ImageJ program (NIH, USA).

## II-3. RT-PCR and Real-time PCR

hBM-MSCs were harvested and the total RNAs were extracted using RNAiso reagent (TAKARA, Japan) according to the manufacturer's instructions. The Primescript II 1$^{st}$ strand cDNA synthesis kit (TAKARA, Japan) was used to reverse transcribe 3-5 μg of total RNA with 0.2 μg of random primers (TAKARA, Japan), 1 mM dNTPs, and the supplied buffer. First strand cDNAs were amplified with *Taq* DNA polymerase (MBI Fermentas, USA) with gene-specific primers for human *Nestin-1*, *Musashi*, *NeuN*, *MAP-2*, *NF-M*, *KCNH5*, or *β-actin*. PCR cycling parameters were as follows: initial denaturation at 94°C for 2 min; 30 cycles of 30 sec at 94°C

for denaturation, 30 sec at 55°C for primer annealing, 30 sec at 72°C for extension, and a final extension at 72°C for 10 min. PCR products were visualized under agarose gel electrophoresis.

For real-time PCR, first strand cDNAs were amplified using the Power SYBR Green PCR master mix (Applied Biosystems Inc., USA) with gene-specific primers for human *Nestin-1*, *Musashi*, *CD133*, *GFAP, Nanog, SDF-1α*, *NeuN*, *MAP-2*, *NF-M*, *KCNH1*, *KCNH5*, *ALP, Adiponectin*, *FABP*4, *MMP*13, or *β-actin*. Real-time PCR cycling parameters were 95°C for 10 min, followed by 40 cycles of 15 sec at 95°C, and 1 min at 58°C. Primers were synthesized by IDT (Integrated DNA Technologies Inc., USA) and are summarized in Table 1. Primers for SDF-1α were purchased from SuperArray Bioscience Corporation (Frederick, MD, USA).

Table 1. Oligonucleotides used for real-time RT-PCR

| Gene | Forward primer (5' → 3') | Reverse primer (5' → 3') | Acc. No. |
|---|---|---|---|
| *Nanog* | GTCCCAAAGGCAAACAACCC | GCTGGGTGGAAGAGAACACA | NM_024865 |
| *Nestin* | AGCCCTGACCACTCCAGTTT | GCTGCTTACCACTTTGCCCT | NM_006617 |
| *Musashi* | ATAAAGTGCTGGCGCAATCG | TCGTTCGAGTCACCATCTTGG | NM_002442 |
| *CD133* | CCTGGGGCTGCTGTTTATTAT | ATTTTCCTTCTGTCGCTGGT | NM_006017 |
| *GFAP* | TGGGAGCTTGATTCTCAGCA | CCTGGGCTTGACCTCTCTGTA | NM_002055 |
| *NeuN* | TGGCATGACCCTGTACACAC | TGCTTCTCTGTAGGGTCGGA | NM_001082575 |
| *MAP-2* | TTGGTGCCGAGTGAGAAGAA | GGTCTGGCAGTGGTTGGTTAA | NM_002374 |
| *NF-M* | GTGAACCACGAGAAGGCTCA | AGGTAGTCTTTGCGCTCCAC | NM_005382 |
| *KCNH1* | TTGGAGATGTGTTCTGGAAGGAA | AGGGCATCCCGCTTGATC | NM_172362.2 |
| *KCNH5* | GACGAAATTTGCCCGATTGA | TGAATGTTTATGGACCACCTCTGT | NM_139318 |
| *β-actin* | ATCCGCAAAGACCTGTACGC | TCTTCATTGTGCTGGGTGCC | NM_001101 |

Acc. No. indicates gene access number.

## Ⅱ-4. Immunocytochemical staining

Differentiated MSCs were stained with neuronal-specific antibodies against Nestin and NF-M. hBM-MSCs were grown on poly-l-lysine-coated coverslips (Fisher Scientific, USA) and induced to differentiate into neuron-like cells. Cells were then fixed with fixation solution containing 4% paraformaldehyde in phosphate-buffered saline (PBS) for 15 min at room temperature (RT). After three washes with 500 μl of PBS, the cells were permeabilized with ice-cold methanol for 5 min at RT. Cells were then washed three times with PBS and incubated with blocking buffer (5% horse serum in PBS containing 0.02% sodium azide) for 1 hour at RT. Cells were incubated with antibodies to NF-M or Nestin (Santa Cruz biotechnology, USA) diluted 1:200 in blocking buffer overnight at 4°C. After three washes in 500 μl of PBS-A (containing 0.02% sodium azide), the cells were incubated with Alexa 488-conjugated donkey anti-goat IgG antibodies (Molecular Probes Inc., USA) diluted 1:500 in Hoechst 33342 (Molecular Probes Inc., USA) for 1 hour at RT, then washed three times with PBS, and mounted with a drop of mounting solution (ProLong Gold antifade reagent, Molecular Probes Inc., USA). The cells were visualized by fluorescence microscopy with a Nikon Eclipse 80Ti microscope (Nikon, Japan). Cell images were taken with a DS-RI1 digital camera (Nikon, Japan).

## Ⅱ-5. Immunoblot analysis

Cells were extracted with 400 μl RIPA buffer containing protease and dephosphatase inhibitors (Santa Cruz Biotechnology, USA) for 30 min at 4°C, and centrifuged at 16,000 x g for 20 min. The total proteins were then subjected to immunoblotting with antibodies to Nestin (1:1000), Musashi (1:1000), CD133 (1:1000), GFAP (1:500), NF-M (1:500), or GAPDH (1:5000), and subsequently the appropriate HRP (horseradish peroxidase)-conjugated secondary antibodies (Jackson ImmunoResearch Laboratories, USA). Western blots were quantified with the ImageJ program.

# III. Results

## III-1. Neuroprogenitor gene markers are induced by VPA in hBM-MSCs

To evaluate the role of VPA in cell fate, hBM-MSCs were incubated with 200 μg/ml VPA for 12 hours according to our previously described procedures [4]. This determined condition of VPA inhibits HDAC, not GSK-3 [9, 10, 16, 21]. The expression of neuroprogenitor markers was measured by real-time PCR. Transcripts of the neuroprogenitor genes *Nestin-1*, *Musashi*, *CD133*, and *GFAP* were significantly increased in VPA-treated hBM-MSCs (VPA-MSCs) while *NANOG* and *SDF-1a* levels were unchanged compared to non-treated hBM-MSCs (ctrl-MSCs; *t*-test, * $p<0.05$, ** $p<0.005$, mean ± SD, n=6) (Fig. 1). Data consistent with these results were obtained from immunoblot analysis (Fig. 1B).

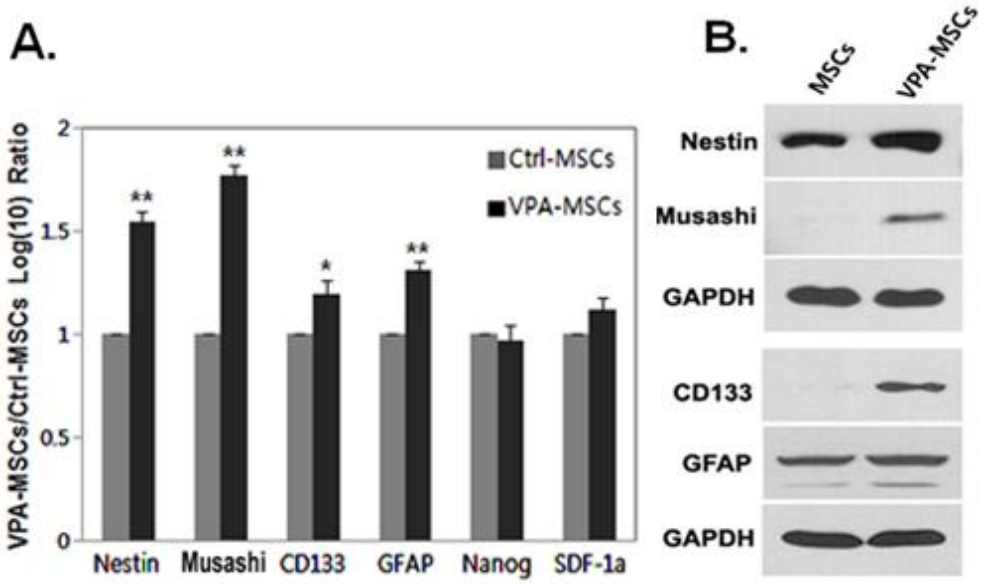
A.
VPA-MSCs/Ctrl-MSCs Log(10) Ratio
2
1.5
1
0.5
0
Ctrl-MSCs
VPA-MSCs
**
**
*
**
Nestin
Musashi
CD133
GFAP
Nanog
SDF-1a
B.
MSCs
VPA-MSCs
Nestin
Musashi
GAPDH
CD133
GFAP
GAPDH

**Figure 1. Neuroprogenitor marker gene expression is induced in VPA-treated hBM-MSCs.**

(A) The expression of neuroprogenitor and stem cell marker genes were measured by real-time PCR. The neuroprogenitor markers, *Nestin*, *Muashi*, *CD*133, and *GFAP* were significantly increased in VPA-treated hBM-MSCs (VPA-MSCs) compared to non-treated hBM-MSCs (ctrl-MSCs; *t*-test, * $p<0.05$, ** $p<0.005$, mean ± SD, n=6). (B) Neuroprogenitor proteins also increased in VPA-MSCs, as measured by immunoblot analysis with antibodies specific to Nestin, Musashi, CD133, and GFAP. GAPDH was used as a standard control.

## III-2. VPA-pretreated hBM-MSCs have a neuronal appearance in neuronal induction media

Since VPA stimulates the expression of neuroprogenitor genes, I hypothesized VPA-MSCs could be more effectively differentiated into neuronal cells than control MSCs (ctrl-MSCs). To evaluate this hypothesis, both MSCs (ctrl- and VPA-MSCs) were differentiated with neuronal induction media. Both neuronal differentiated MSCs (Fig. 2A; dMSCs and VPA-dMSCs) exhibited a neuronal morphology, while undifferentiated BM-MSCs (ctrl-MSCs) and VPA-MSCs showed a flattened and spindle-shaped appearance similar to primary hBM-MSCs (Fig. 2A, ctrl-MSCs and VPA-MSCs). Estimating the rate of neuronal differentiation in VPA-dMSCs and dMSCs, VPA-dMSCs significantly differentiated into neuron-like cells compared to dMSCs (Fig. 2B and Table 2; *t*-test, # $p<0.01$, mean ± SD, n=4). The average neurite length of dMSCs was also significantly extended in VPA-dMSCs (Fig. 2C and Table 3; *t*-test, * $p<0.05$ mean ± SD, n=4); however, a significant difference in the number of neurites was not observed for dMSCs or VPA-dMSCs (Fig. 2D and Table 3).

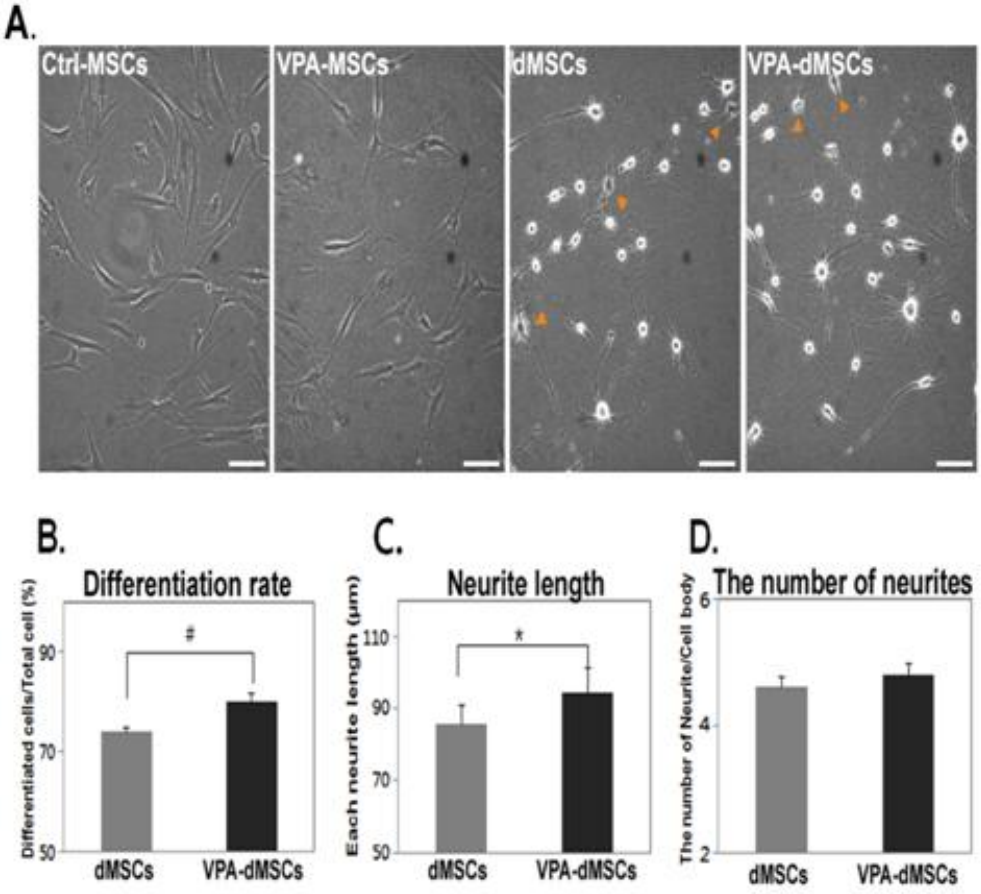
A.
Ctrl-MSCs
VPA-MSCs
dMSCs
VPA-dMSCs
B.
Differentiation rate
Differentiated cells/Total cell (%)
90
70
50
#
dMSCs
VPA-dMSCs
C.
Neurite length
Each neurite length (μm)
110
90
70
50
*
dMSCs
VPA-dMSCs
D.
The number of neurites
The number of Neurite/Cell body
6
4
2
dMSCs
VPA-dMSCs

**Figure 2. Neuron-like morphological changes in VPA-pretreated hBM-MSCs followed by neuronal induction.**

(A) Both ctrl-MSCs and VPA-MSCs differentiated into neuronal cells following exposure to neuronal induction media. Differentiated MSCs are indicated in dMSCs and VPA-dMSCs. Yellow arrowheads indicate undifferentiated MSCs. Scale bar indicates 100 μm. (B) Total cells and neuronal-shaped cells were counted to estimate the neuronal differentiated rate. VPA-dMSCs were significantly differentiated compared to dMSCs (*t*-test, # $p<0.01$, mean ± SD, n=4). (C) The neurite length of differentiated cells was significantly extended in VPA-dMSCs (Fig. 2C and 2D; *t*-test, * $p<0.05$ mean ± SD, n=4). (D) The number of neurites in differentiated cells did not significantly increase.

Table 2. The neuron-like cells were counted to estimate the neuronal differentiation rate

| **Experiments** (n=4) | **dMSCs** (Neuron-like cells / Total cells) | **VPA-dMSCs** (Neuron-like cells / Total cells) |
|---|---|---|
| **1st** | 91 / 118 (77.1 %) | 91 / 108 (84.3 %) |
| **2nd** | 234 / 321 (72.9 %) | 241 / 309 (78 %) |
| **3rd** | 171 / 234 (73 %) | 432 / 557 (77.6 %) |
| **4th** | 586 / 806 (72.7 %) | 578 / 713 (81.1 %) |
| **Sum** | 1082 / 1479 (73.9 ± 3 %) | 1342 / 1687 (80.25 ± 3 %) |

Table 3. The number of neurites from each differentiated cells were counted and neurite lengths were measured.

| dMSCs | | | |
|---|---|---|---|
| **Experiments (n=4)** | **Total cells** | **The No. of Neurite (Ave/each cell)** | **Neurite length (Ave/each neurite, ㎛)** |
| **1st** | 36 | 5.14 | 104.22 |
| **2nd** | 45 | 4.54 | 120 |
| **3rd** | 45 | 4.43 | 89.91 |
| **4th** | 70 | 4.34 | 117.7 |
| **Ave.** | 49 | 4.61 | 107.96 |

| dMSCs | | | |
|---|---|---|---|
| **Experiments (n=4)** | **Total cells** | **The No. of Neurite (Ave/each cell)** | **Neurite length (Ave/each neurite, ㎛)** |
| **1st** | 36 | 5.06 | 120.19 |
| **2nd** | 45 | 4.72 | 133.24 |
| **3rd** | 45 | 7.82 | 92.74 |
| **4th** | 70 | 4.16 | 129.42 |
| **Ave.** | 49 | 4.69 | 118.9 |

## III-3. Significant increases in the expression of diverse neuronal markers in VPA-dMSCs

Since VPA-dMSCs have neuronal appearances, the expression of various neuronal-specific marker genes was evaluated by RT-PCR and real-time PCR (Fig. 3A and 3B). All genes tested in this study were significantly increased in either VPA-dMSCs and dMSCs compared to undifferentiated MSCs (ctrl-MSCs) (Fig. 3B; *t*-test, * $p<0.001$, mean ± SD, n=7). The transcripts of neuronal-specific marker genes (*MAP-2, NF-M*, *KCNH2*, and *KCNH5*) significantly increased in VPA-dMSCs compared to dMSCs (Fig. 3B; *t*-test, # $p<0.02$, ## $p<0.01$, mean ± SD, n=7). I also examined the expression of other lineage specific markers in dMSCs and VPA-dMSCs, and identified the decreased expressions of osteogenic (*ALP*), adipogenic (*Adiponectin*, *FABP*4) and chondrogenic (*MMP*13) specific genes in compared to ctrl-MSCs (Fig. 3C; mean ± SD, n=3).

.

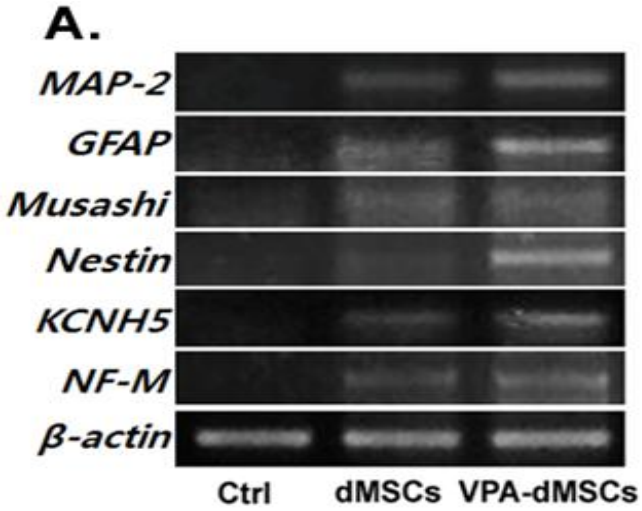
A.
MAP-2
GFAP
Musashi
Nestin
KCNH5
NF-M
β-actin
Ctrl
dMSCs
VPA-dMSCs

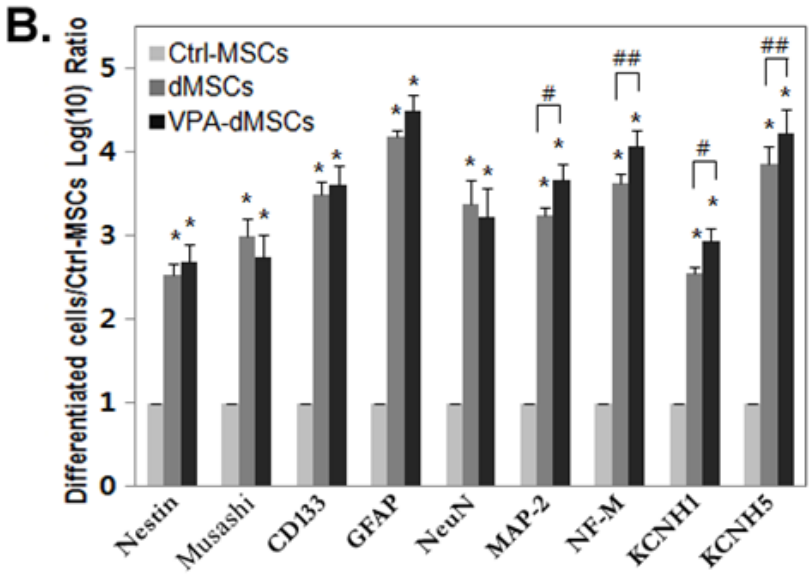
B.
Ctrl-MSCs
dMSCs
VPA-dMSCs
Differentiated cells/Ctrl-MSCs Log(10) Ratio
0
1
2
3
4
5
Nestin
Musashi
CD133
GFAP
NeuN
MAP-2
NF-M
KCNH1
KCNH5

C.

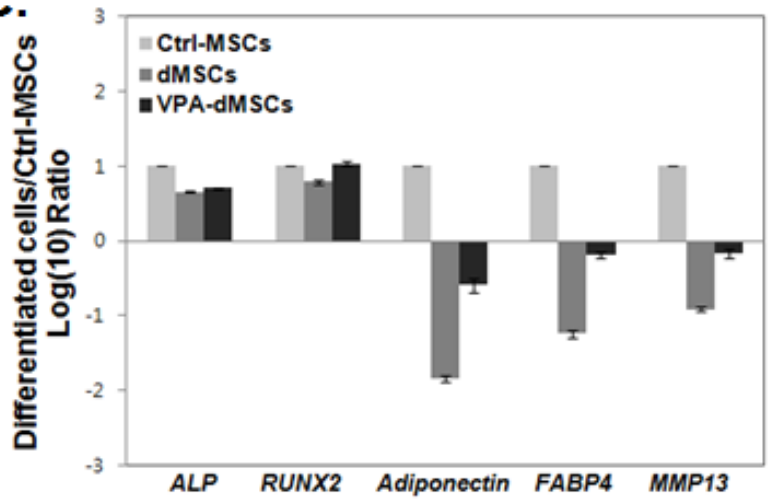
Differentiated cells/Ctrl-MSCs
Log(10) Ratio
Ctrl-MSCs
dMSCs
VPA-dMSCs
3
2
1
0
-1
-2
-3
ALP
RUNX2
Adiponectin
FABP4
MMP13

**Figure 3. Diverse neuronal markers are increased in differentiated VPA-MSCs.**

The expression of several neuronal specific genes were measured in MSCs (ctrl-MSCs) and differentiated MSCs (dMSCs, VPA-dMSCs) by RT-PCR (A) and real-time PCR (B). All genes tested in this experiment significantly increased in differentiated MSCs (*t*-test, * $p<0.001$, mean ± SD, n=7). *MAP-2*, *NF-M*, *KCNH1*, and *KCNH5* significantly increased in VPA-dMSCs compared to dMSCs (*t*-test, # $p<0.02$, ## $p<0.01$, mean ± SD, n=7). (C) The expressions of osteogenic, adipogenic and chondrogenic specific genes were decreased in both dMSCs and VPA-dMSCs compared to ctrl-MSCs (mean ± SD, n=3).

## III-4. Neuronal-specific proteins are upregulated in VPA-dMSCs

To characterize the neuronal differentiation observed at a protein level, I used immunocytochemical staining. Ctrl-MSCs, VPA-dMSCs and dMSCs were fixed and stained with specific antibodies against the neuronal marker proteins NF-M and Nestin. Neuronal-induced MSCs, dMSCs, and VPA-dMSCs exhibited positive cytoplasmic staining for both NF-M and Nestin in contrast to non-induced MSCs (ctrl-MSCs, Fig. 4A). Consistent results were obtained from immunoblot analysis using antibodies specific to NF-M, and Nestin (Fig. 4B).

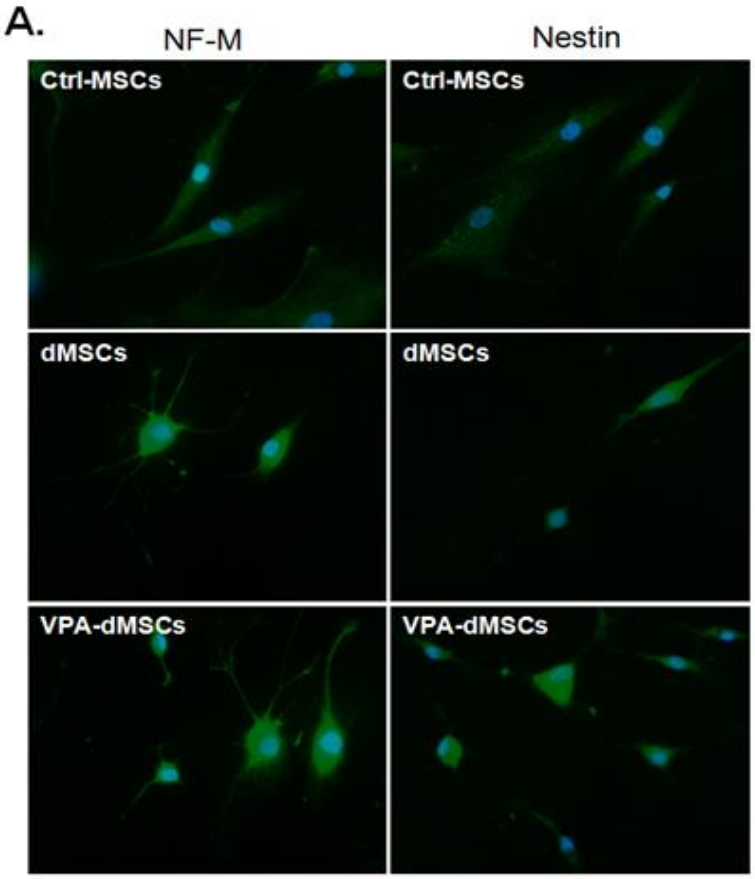
A.
NF-M
Nestin
Ctrl-MSCs
Ctrl-MSCs
dMSCs
dMSCs
VPA-dMSCs
VPA-dMSCs

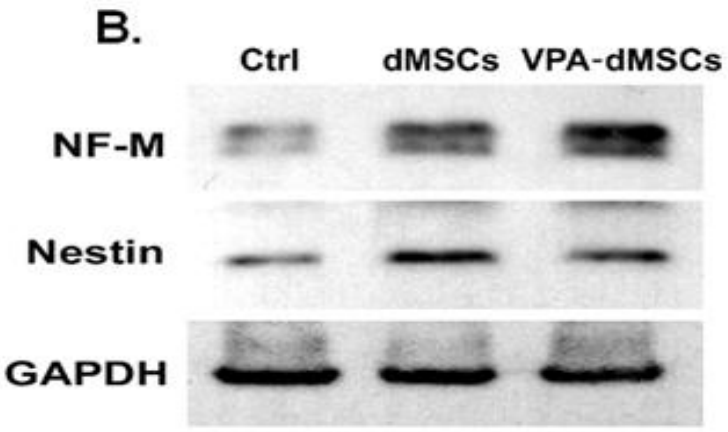
B.
Ctrl
dMSCs
VPA-dMSCs
NF-M
Nestin
GAPDH

Figure 4. Upregulation of NF-M and Nestin in VPA-dMSCs.

(A) MSCs (ctrl-MSCs) and differentiated MSCs (dMSCs and VPA-dMSCs) were fixed and stained with antibodies against the neuronal specific markers NF-M (left panel) and Nestin (right panel), and visualized under fluorescent microscopy. (B) Consistent results were obtained from immunoblot analysis. GAPDH was used as an internal standard.

# IV. Discussion

Our previous study showed that VPA (given at an optimal dose and incubation time) stimulates the secretion of various trophic factors from hBM-MSCs, which may improve the efficacy of stem cell therapy [4]. Other recent studies have provided evidence that HDAC inhibitors enhance stem cell differentiation [13, 18, 27, 32], suggesting VPA may confer a differential potency to stem cells. In this study, VPA treatment significantly increased the expression of the neuronal progenitor genes *Nestin*-1, *Musashi*, *CD133*, and *GFAP* in hBM-MSCs (Fig. 1A). This was further confirmed through an immunoblot analysis (Fig. 1B). These results indicate effective neuronal differentiation in VPA-treated MSCs.

VPA induces the neuronal differentiation of adult hippocampal neural progenitors [12]. Other groups have reported that VPA induces hippocampal neurogenesis and the acetylation of histone 4 [32]. In this study, I examined whether hBM-MSCs effectively differentiate into neuronal cells following VPA pre-incubation, and found a significant increase in the differentiation rate of VPA-pretreated BM-MSCs (Fig. 2A and 2B). Neurite lengths were also significantly extended in VPA-dMSCs (Fig. 2C). These cells significantly increased their transcripts for all neuronal-specific markers tested in both differentiated MSCs (Fig. 3). The gene expression

of *MAP-2* (dendritic marker) [14], *NF-M*, and the neural specific calcium channels *KCNH2* and *KCNH5*, significantly increased in VPA-pretreated dMSCs compared to dMSCs (Fig. 3). This suggests VPA-MSCs are more effectively differentiated into neuron-like cells than ctrl-MSCs in the presence of neuronal induction media.

Inhibition of histone deacetylation by VPA is associated with an open chromatin conformation (called euchromatin) resulting in transcriptional activation at gene loci [7, 24]. HDAC inhibitors reversible this functional activity and withdrawal of the inhibitor may return chromatin to a closed conformation (called heterochromatin) [6]. However, some neuronal-specific genes which are epigenetically activated may partially prevent this return to the inactive form in the presence of neuronal induction media [24]. This suggests that the timing of HDAC inhibitor treatment is critical for inducing effective cell differentiation. In this study, I studied different timepoints for VPA treatment in neuronal differentiation and found VPA pre-incubation prior to neuronal induction effectively induces neuronal differentiation in BM-MSCs (Figs. 2 and 3). The neuronal differentiated MSCs (dMSCs) were confirmed at the protein level, using immunocytochemical staining and immunoblot analysis with antibodies targeting NF-M and Nestin proteins, and upregulation of these proteins was observed for both neuronal differentiated MSCs and VPA-pretreated

ones (Fig. 4A and 4B).

I have shown that VPA pretreatment of BM-MSCs effectively stimulates neuronal differentiation. However, which gene locus is directly involved in this modification has not been confirmed. Based on the functional mechanism of VPA as a histone deacetylase inhibitor, VPA induces histone acetylation on chromatin, resulting in the activation of several gene loci and regulating gene expression [7]. Since VPA has been pharmacologically applied to neurological diseases for several decades, some VPA-induced genes may be functionally active in stem cell differentiation, especially neuronal differentiation. Previous studies have shown that HDAC inhibitors enhances the differentiation capacity of stem cells [13, 18, 27, 32]. Here, I have shown that the HDAC inhibitor VPA stimulates the differentiation of BM-MSCs into neuron-like cells through the simple pre-incubation of VPA.

BM-MSCs have the potential to differentiate into neurons [31], making them an excellent candidate for stem cell therapy in a neurodegenerative disease. However, only a few cells among the transplanted MSCs are differentiated into neuronal cells in vivo study. It suggests that the differentiation potency of stem cells need to be improved prior to implantation. In this study, I have shown that VPA promotes neuronal differentiation by induction of neuroprogenitors in hBM-MSCs and suggests that VPA pretreatment of MSCs may give better efficacy in

neurodegenerative diseases.

This study has demonstrated that VPA-treated MSCs endogenously induce the expression of neuroprogenitor marker genes that synergistically promote neuronal differentiation in the presence of neuronal induction media. VPA-pretreated MSCs may thus enhance neuronal differentiation and provide advances in stem cell therapy for neurodegenerative disorders.

# V. References


[1] J.E. Bolden, M.J. Peart, R.W. Johnstone, Anticancer activities of histone deacetylase inhibitors, Nat Rev Drug Discov 5 (2006) 769-784.

[2] A.I. Caplan, Adult mesenchymal stem cells for tissue engineering versus regenerative medicine, J Cell Physiol 213 (2007) 341-347.

[3] S.M. Chambers, C.A. Shaw, C. Gatza, C.J. Fisk, L.A. Donehower, M.A. Goodell, Aging hematopoietic stem cells decline in function and exhibit epigenetic dysregulation, PLoS Biol 5 (2007) e201.

[4] G.W. Cho, B.Y. Kang, K.S. Kim, S.H. Kim, Effects of valproic acid on the expression of trophic factors in human bone marrow mesenchymal stromal cells, Neurosci Lett 526 (2012) 100-105.

[5] G.W. Cho, M.Y. Noh, H.Y. Kim, S.H. Koh, K.S. Kim, S.H. Kim, Bone marrow-derived stromal cells from amyotrophic lateral sclerosis patients have diminished stem cell capacity, Stem Cells Dev 19 (2010) 1035-1042.

[6] M. Dokmanovic, C. Clarke, P.A. Marks, Histone deacetylase inhibitors: overview and perspectives, Mol Cancer Res 5 (2007) 981-989.

[7] W. Fischle, Y. Wang, C.D. Allis, Binary switches and modification cassettes in histone biology and beyond, Nature 425 (2003) 475-479.

[8] M. Gabbianelli, U. Testa, A. Massa, E. Pelosi, N.M. Sposi, R. Riccioni, L. Luchetti, C. Peschle, Hemoglobin switching in unicellular erythroid culture of sibling erythroid burst-forming units: kit ligand induces a dose-dependent fetal hemoglobin reactivation potentiated by sodium butyrate, Blood 95 (2000) 3555-3561.

[9] M. Gottlicher, S. Minucci, P. Zhu, O.H. Kramer, A. Schimpf, S. Giavara, J.P. Sleeman, F. Lo Coco, C. Nervi, P.G. Pelicci, T. Heinzel, Valproic acid defines a novel class of HDAC inhibitors inducing differentiation of transformed cells, EMBO J 20 (2001) 6969-6978.

[10] N. Gurvich, O.M. Tsygankova, J.L. Meinkoth, P.S. Klein, Histone deacetylase is a target of valproic acid-mediated cellular differentiation, Cancer Res 64 (2004) 1079-1086.

[11] P.M. Haddad, A. Das, M. Ashfaq, A. Wieck, A review of valproate in psychiatric practice, Expert Opin Drug Metab Toxicol 5 (2009) 539-551.

[12] J. Hsieh, K. Nakashima, T. Kuwabara, E. Mejia, F.H. Gage, Histone deacetylase inhibition-mediated neuronal differentiation of multipotent adult neural progenitor cells, Proc Natl Acad Sci U S A 101 (2004) 16659-16664.

[13] S. Iezzi, M. Di Padova, C. Serra, G. Caretti, C. Simone, E. Maklan, G.

Minetti, P. Zhao, E.P. Hoffman, P.L. Puri, V. Sartorelli, Deacetylase inhibitors increase muscle cell size by promoting myoblast recruitment and fusion through induction of follistatin, Dev Cell 6 (2004) 673-684.

[14] M. Iwata, K.T. Muneoka, Y. Shirayama, A. Yamamoto, R. Kawahara, A study of a dendritic marker, microtubule-associated protein 2 (MAP-2), in rats neonatally treated neurosteroids, pregnenolone and dehydroepiandrosterone (DHEA), Neurosci Lett 386 (2005) 145-149.

[15] C.U. Johannessen, Mechanisms of action of valproate: a commentatory, Neurochem Int 37 (2000) 103-110.

[16] W. Jonathan Ryves, E.C. Dalton, A.J. Harwood, R.S. Williams, GSK-3 activity in neocortical cells is inhibited by lithium but not carbamazepine or valproic acid, Bipolar Disord 7 (2005) 260-265.

[17] J. Koch-Weser, T.R. Browne, Drug therapy: Valproic acid, N Engl J Med 302 (1980) 661-666.

[18] P. Marianna, P. Kollia, S. Akel, Y. Papassotiriou, A. Stamoulakatou, D. Loukopoulos, Valproic acid, trichostatin and their combination with hemin preferentially enhance gamma-globin gene expression in human erythroid liquid cultures, Haematologica 86 (2001) 700-705.

[19] G.C. Minetti, C. Colussi, R. Adami, C. Serra, C. Mozzetta, V. Parente, S. Fortuni, S. Straino, M. Sampaolesi, M. Di Padova, B. Illi, P. Gallinari, C. Steinkuhler, M.C. Capogrossi, V. Sartorelli, R. Bottinelli, C. Gaetano, P.L. Puri, Functional and morphological recovery of dystrophic muscles in mice treated with deacetylase inhibitors, Nat Med 12 (2006) 1147-1150.

[20] S. Minucci, P.G. Pelicci, Histone deacetylase inhibitors and the promise of epigenetic (and more) treatments for cancer, Nat Rev Cancer 6 (2006) 38-51.

[21] C.J. Phiel, F. Zhang, E.Y. Huang, M.G. Guenther, M.A. Lazar, P.S. Klein, Histone deacetylase is a direct target of valproic acid, a potent anticonvulsant, mood stabilizer, and teratogen, J Biol Chem 276 (2001) 36734-36741.

[22] M.F. Pittenger, A.M. Mackay, S.C. Beck, R.K. Jaiswal, R. Douglas, J.D. Mosca, M.A. Moorman, D.W. Simonetti, S. Craig, D.R. Marshak, Multilineage potential of adult human mesenchymal stem cells, Science 284 (1999) 143-147.

[23] M.A. Rogawski, W. Loscher, The neurobiology of antiepileptic drugs, Nat Rev Neurosci 5 (2004) 553-564.

[24] N. Sengupta, E. Seto, Regulation of histone deacetylase activities, J Cell Biochem 93 (2004) 57-67.

[25] R. Shahien, S.A. Saleh, A. Bowirrat, Intravenous sodium valproate aborts migraine headaches rapidly, Acta Neurol Scand 123 (2011) 257-265.

[26] A.G. Smith, Embryo-derived stem cells: of mice and men, Annu Rev Cell Dev Biol 17 (2001) 435-462.

[27] R.A. Swank, E. Skarpidi, T. Papayannopoulou, G. Stamatoyannopoulos, The histone deacetylase inhibitor, trichostatin A, reactivates the developmentally silenced gamma globin expression in somatic cell hybrids and induces gamma gene expression in adult BFUe cultures, Blood Cells Mol Dis 30 (2003) 254-257.

[28] T. Thatava, B. Ma, M. Rohde, H. Mayer, Chromatin-remodeling factors allow differentiation of bone marrow cells into insulin-producing cells, Stem Cells 24 (2006) 2858-2867.

[29] G. Van Zant, Y. Liang, The role of stem cells in aging, Exp Hematol 31 (2003) 659-672.

[30] I.L. Weissman, D.J. Anderson, F. Gage, Stem and progenitor cells: origins, phenotypes, lineage commitments, and transdifferentiations, Annu Rev Cell Dev Biol 17 (2001) 387-403.

[31] D. Woodbury, E.J. Schwarz, D.J. Prockop, I.B. Black, Adult rat and human bone marrow stromal cells differentiate into neurons, J Neurosci Res 61 (2000) 364-370.

[32] I.T. Yu, J.Y. Park, S.H. Kim, J.S. Lee, Y.S. Kim, H. Son, Valproic acid promotes neuronal differentiation by induction of proneural factors in association with H4 acetylation, Neuropharmacology 56 (2009) 473-480.

# I. Introduction

Bone marrow-mesenchymal stromal cells (BM-MSCs) possess the capacities to differentiate into variety of cell types [1], such as adipocyte, chondrocyte, osteocyte and neurocyte [2]. MSCs also secrete diverse trophic factors which provide the protected environment against oxidative stress and inflammation [3, 4]. These suggest that BM-MSCs are excellent candidate for stem cell therapy. However, stem cells therapies have different efficacy according to the health state and age of donor [5-7]. Previous study has showed that migration and adhesion were markedly decreased at the engraftment of the progenitor cells obtained from unhealthy donors [8, 9]. And also, the increment of intracellular ROS by oxidative stress could lead to progressive functional decline of MSCs for long-term *in vitro* culture [10]. These studies indicate that applied stem cells need to be improved their capacities.

Reactive oxygen species (ROS) was increased in the ischemic injured tissues and induced apoptosis of the transplanted MSCs in stem cell therapy [11]. The adhesion of engraft stem cells play a key role for improvement of efficacy because the attached stem cells at target tissues may have better chance to survive. Recent studies have shown that the ROS productions from injured tissues were disrupted the fibroblast adhesion by impairment of integrin contacts [12]. Thus, the imbalance of

intracellular ROS by chronic oxidative stress could lead to functional decline and progress the cell senescence [13].

Histone deacetylases (HDACs) play a key role for mediating diverse gene expressions by regulation of chromatin modulation proteins [14, 15]. Histone deacetylase (HDAC) inhibitors have been applied in various diseases such as cancer [15], mood disorder [16] and neurodegenerative disorder [17]. Recent studies have shown that HDAC inhibitor, trichostatin A (TSA), applied strategy of treatment for reducing brain injury following cerebral ischemia [18]. Another HDAC inhibitor, valproic acid (VPA), has been generally used for the treatment of epilepsy [19, 20] and bipolar disorder [21, 22]. Therefore, the usage of HDAC inhibitors could provide an increase therapeutic efficacy in these patients.

Trichostatin A (TSA) is known as Histone deacetylases (HDACs) inhibitor [23] which selectively inhibits class I and II HDACs in the low molar concentration. Recent study reported that TSA was improved survival and delays disease progression in mouse model of amyotrophic lateral sclerosis (ALS) [24]. Another study has been reported that TSA has protective effects for cisplatin-induced ototoxicity through the regulation of apoptosis inducing genes [25]. It provides that TSA might be strong candidates for increasing the protective capacities of cells against oxidative stress.

In this study, I investigated whether TSA regulates the levels of intracellular ROS in human BM-MSCs, and identified the reduction of intracellular ROS production and cytotoxicity against oxidative stress.

# II. Materials and Methods

## II-1. Characteristics of primary human BM-MSCs and cell culture

hBM-MSCs were puschased from CEFO (Cell Engineering For Origin, Korea). The viral infection and mycoplasma contamination were presented all negative in cells. Flow cytometric analysis of the cells revealed a $CD73^+$, $CD105^+$, $CD31^-$ phenotype. The hBM-MSCs were cultured in T75 flask (Becton Dickinson, USA) according to the supplier's recommendations. Cells were cultivated in hBM-MSC growth media (Gibco, USA), containing the mesenchymal cell growth supplements, L-glutamine, penicillin, and streptomycin, without any stimulatory supplements or vitamins. Cells were maintained in a humidified incubator at 37 °C, using a standard mixture of 95% air and 5% $CO_2$. MSCs passaged seven times were used.

## II-2. MTT assay

To evaluate the protective effects of TSA against $H_2O_2$- or SA-induced oxidative stress, the viabilities of TSA-treated MSCs were measured by MTT assay (Sigma, USA) according to the manufacturer's instructions. Briefly, 8 x $10^3$ hBM-MSCs were seeded onto 96-well plates. Next day, the cells were incubated with/without 200 nM of TSA for 8 hours and then cells were treated with 0 ~ 3 mM $H_2O_2$ for 1 hour and subjected to MTT assay. Data are presented as means ± SD from three independent

experiments. Statistical comparisons between groups were conducted by student *t*-test.

## II-3. Detection of intracellular ROS

Intracellular ROS levels in the treated MSCs were measured using the cell permeable substrate, 2',7'-Dichlorofluorescin diacetate (DCFH-DA), which is converted to the fluorescent product, 2',7'-dichlorodihydrofluorescein (DCF). Cells were seeded in 24-well plates and incubated with 20 μM DCFH-DA at 37 °C for 1 hour and then incubated with trichostatin A (TSA) for 8 hours at 37 °C. After washing with PBS two times, the cells were incubated with $H_2O_2$ (0.5 mM ~ 3mM) or sodium arsenite (0.5 mM ~ 1.5 mM) for 1hour at 37 °C. The cells were then visualized under the fluorescence microscopy (a Nikon Eclipse 80Ti microscope, Nikon, Japan). Cell images were taken with a DS-Ri1 digital camera (Nikon, Japan)

# III. Results

## III-1. Increment of reactive oxygen species in human BM-MSCs treated with hydrogen peroxide or sodium arsenite

To examine intracellular ROS change by oxidative stress, I performed DCFH-DA assay for ROS detection in hBM-MSCs treated with $H_2O_2$ (0.5 mM ~ 3 mM) or sodium arsenite (SA, 0.5 mM ~ 1.5 mM) for 1 hour. The intracellular ROS were significantly increased in $H_2O_2$ treated MSCs ($H_2O_2$-MSCs) and SA treated MSCs (SA-MSCs) compared with non-treated MSCs (Ctrl-MSCs) (Fig. 1A). ROS-positive cells in each group were counted. The intracellular ROS levels were increased in a dose dependent manner in $H_2O_2$- or SA-treated MSCs (Fig. 1B). To evaluate the viability in stress induced hBM-MSCs, I used a MTT assay. The cell viabilities were gradually decreased following by the treatment of $H_2O_2$ or SA in hBM-MSCs (Fig. 1C). These results suggest that the viability of hBM-MSCs is affected by intracellular ROS induced by oxidative stress.

A.

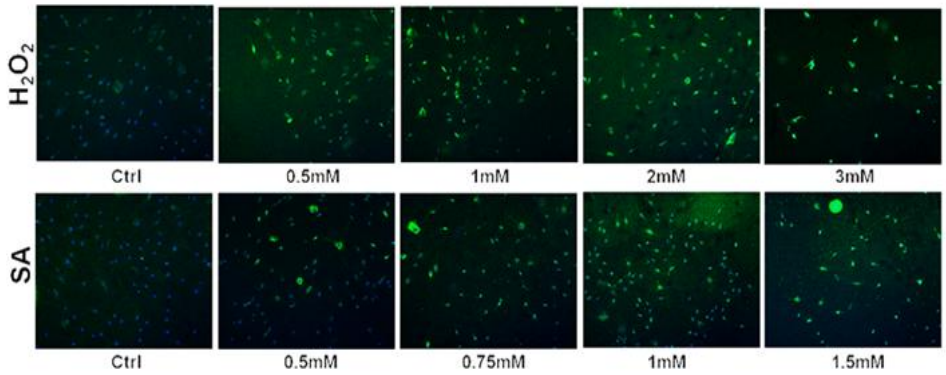
$H_2O_2$
Ctrl
0.5mM
1mM
2mM
3mM
SA
Ctrl
0.5mM
0.75mM
1mM
1.5mM

B.

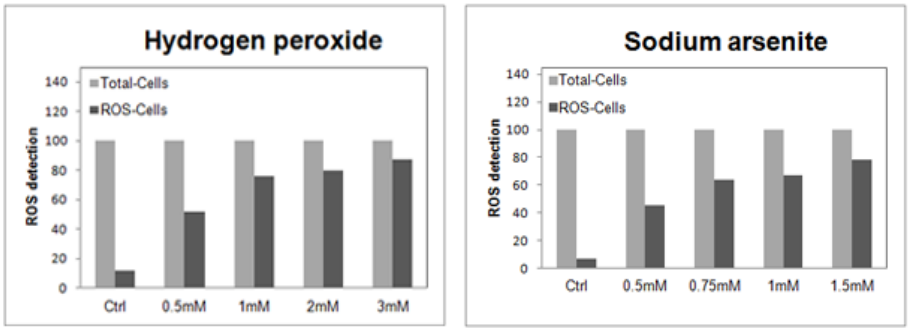
Hydrogen peroxide
Total-Cells
ROS-Cells
ROS detection
0
20
40
60
80
100
120
140
Ctrl
0.5mM
1mM
2mM
3mM
Sodium arsenite
Total-Cells
ROS-Cells
ROS detection
0
20
40
60
80
100
120
140
Ctrl
0.5mM
0.75mM
1mM
1.5mM

C.

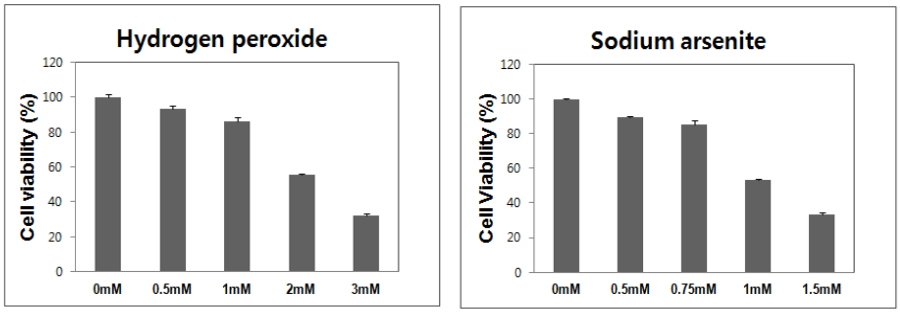
Hydrogen peroxide
Cell viability (%)
0
20
40
60
80
100
120
0mM
0.5mM
1mM
2mM
3mM
Sodium arsenite
Cell Viability (%)
0
20
40
60
80
100
120
0mM
0.5mM
0.75mM
1mM
1.5mM

Figure 1. Increment of reactive oxygen species by treatment of hydrogen peroxide or sodium arsenite in human BM-MSCs.

(A) Intracellular ROS levels were visualized by fluorescence microscope followed by treatment with $H_2O_2$ (0.5 mM to 3 mM) or sodium arsenite (SA, 0.5 mM to 1.5 mM) for 1 hour. The intracellular ROS were significantly increased in $H_2O_2$ treated MSCs ($H_2O_2$-MSCs) and sodium arsenite treated MSCs (SA-MSCs) compared with non-treated MSCs (Ctrl-MSCs). (B) Total cells and ROS induced cells (ROS-MSCs) were counted to estimate the rate of ROS induced MSCs. (C) Cell viabilities with $H_2O_2$-MSCs (upper panels) and SA-MSCs (lower panels) were examined by MTT assays.

## III-2. Significant decrement of the intracellular ROS in TSA treated MSCs

To confirm whether $H_2O_2$-induced intracellular ROS are regulated by TSA in hBM-MSCs, I investigated the effects of the TSA against ROS generation. The cells were incubated with TSA (100 nM ~ 1000 nM) for 8 hours, and then treated with $H_2O_2$ at 1mM. The intracellular ROS levels were detected by DCFH-DA. In TSA pretreated MSCs (TSA-MSCs, 100 nM ~ 500 nM), ROS levels were significantly decreased compared to ctrl-MSCs. In contrast, when the cells were incubated with TSA at 1000 nM, the decrement of ROS levels did not observed (Fig. 2A, 2B). These data show that TSA effectively reduced intracellular ROS in hBM-MSCs.

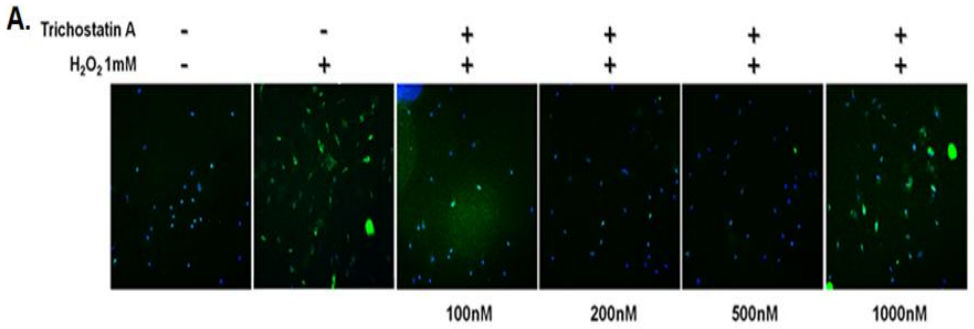
A.
Trichostatin A - - + + + +
H2O2 1mM - + + + + +
100nM
200nM
500nM
1000nM

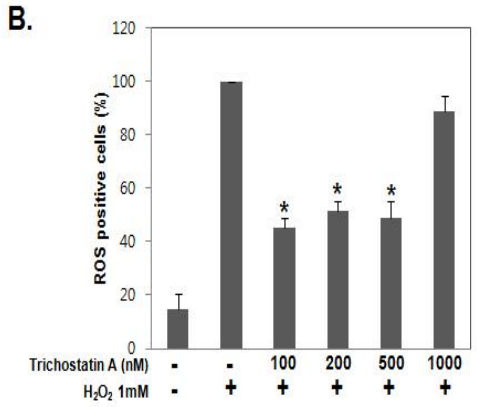
B.
ROS positive cells (%)
120
100
80
60
40
20
0
*
*
*
Trichostatin A (nM) - - 100 200 500 1000
H2O2 1mM - + + + + +

Figure 2. Significant decrement of intracellular ROS in TSA-MSCs.

(A) Cells were incubated with TSA (100 nM to 1000 nM) for 8 hours, and Then treated with 1 mM $H_2O_2$ for 1 hour. The intracellular ROS in TSA-MSCs (100 nM to 500 nM) were significantly decreased compared with $H_2O_2$-MSCs. However, a significant difference in 1000 nM TSA treated MSCs was not observed for $H_2O_2$-MSCs. (B) ROS positive cells per total cells were counted. (*t*-test, * $p<0.05$, mean ± SD, n=3)

## III-3. TSA alone does not contribute to change of ROS levels under condition without oxidative stress

To evaluate cell viability and ROS levels change by TSA treatment alone under the same condition used in figure 2, I performed DCFH-DA and MTT assay in TSA-MSCs. The cells were incubated with TSA (100 ~ 5000 nM) for 8 hours. And then alterations of cell viability and ROS levels were observed. When hBM-MSCs were incubated with TSA (0 ~ 5000 nM) for 8 hours, cell viability and ROS levels were not changed compared to Ctrl-MSCs (Fig. 3A, 3B). From these data, TSA treatment did not affect any toxicity in hBM-MSCs.

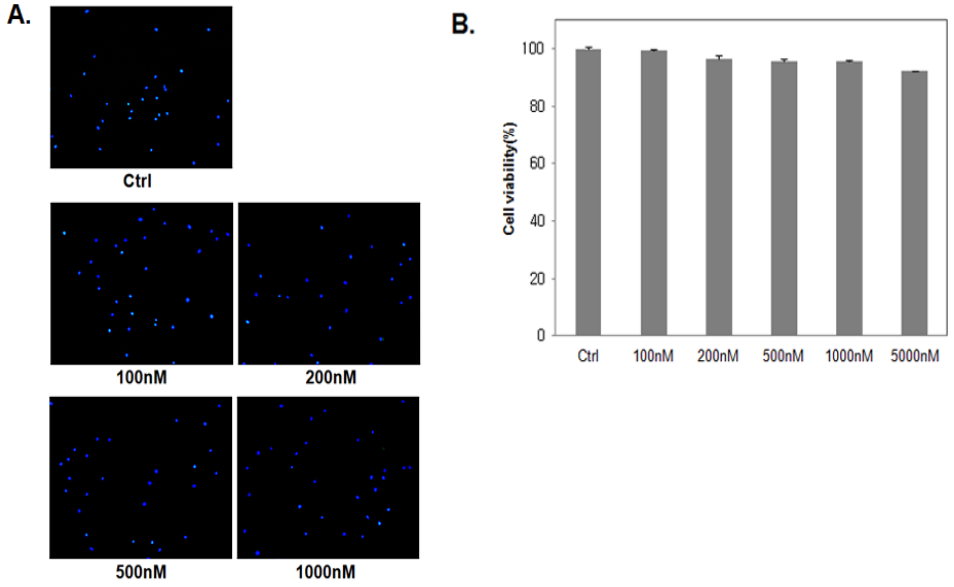
A.
Ctrl
100nM
200nM
500nM
1000nM
B.
Cell viability(%)
100
80
60
40
20
0
Ctrl
100nM
200nM
500nM
1000nM
5000nM

Figure 3. TSA alone does not contribute to change of ROS levels under condition without oxidative stress

(A) After treated with TSA (100 nM to 5000 nM) alone for 8 hours, intracellular ROS levels were visualized by fluorescence microscope. The intracellular ROS in TSA treated MSCs (TSA-MSCs) were not significantly changed compared with non-treated MSCs (Ctrl-MSCs). (B) TSA treatment (0 ~ 5 μM TSA for 8 hours) did not affect any toxicities in hBM-MSCs. (n=3)

## III-4. TSA prevents cellular damage in hBM-MSCs

Previous study reported that increase in ROS could lead to apoptosis [25-27]. To investigate cell apoptosis related to ROS were reduced by TSA treatment, I measured cell viability of hBM-MSCs treated with/without $H_2O_2$ (0.5 ~ 3 mM) after pretreatment of TSA for 8 hours. The viabilities of TSA-MSCs were significantly increased compared with ctrl-MSCs (Fig. 4). This result present that cellular damage due to oxidative stress were reduced by TSA treatment.

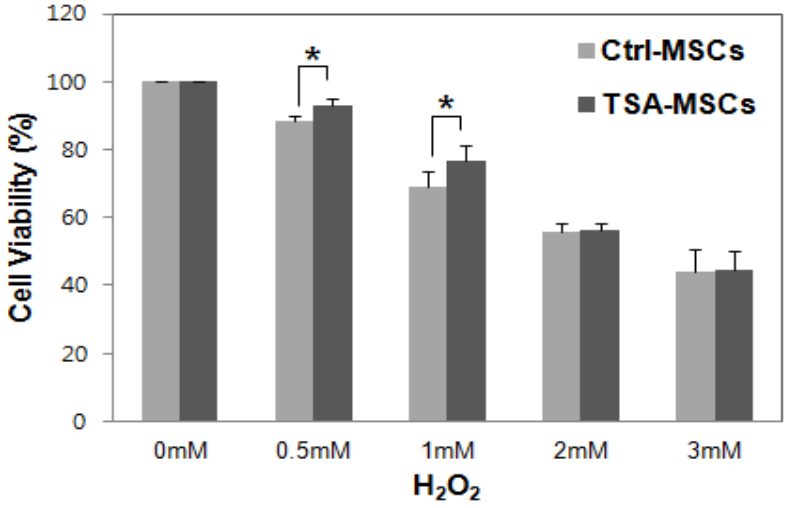
120
100
80
60
40
20
0
Cell Viability (%)
*
*
Ctrl-MSCs
TSA-MSCs
0mM
0.5mM
1mM
2mM
3mM
H2O2

Figure 4. TSA prevents cellular damage in hBM-MSCs

TSA treated hBM-MSCs (200nM of TSA for 8 hours) were treated with 0, 0.5, 1, 2, or 3 mM $H_2O_2$ for 1 hour, and their viabilities were determined by the MTT assay. (*t*-test, $P < 0.05$, mean ± SD, n = 3)

# IV. Discussion

Recently many studies have shown that intracellular ROS have closely related with cellular senescence including functional decline and progression of cell death [10, 13, 28]. In the stem cell therapy, engraft cells were often damaged by ROS. As a results, transplantation efficiency were markedly decrease [8-10]. In this study, I examined the level of intracellular ROS in BM-MSCs which were exposed to hydrogen peroxide ($H_2O_2$) or sodium arsenite (SA). I have observed the dose dependent increase in intracellular ROS during MSCs incubated with $H_2O_2$- or SA- (Fig. 1A and 1B). The cell viabilities were decreased with increase in ROS (Fig. 1C), which is consistent with previous studies [11, 28]. These suggest that applied stem cells need to be improved for protective capacities against harmful factors such as oxidative stress and inflammation.

Previous studies have provided that HDAC inhibitors improve therapeutic efficacy in several disease, such as ischemic stroke [29], cancer [15], mood disorder [16], and neurodegenerative disorder [17]. TSA as well known HDAC inhibitor reduce cellular damage by alcohol-induced toxicity [30], and also present protective effects from cellular toxicity while suppressing of inflammatory pathway [24]. For these reason,

TSA might be an excellent candidate for cell protection against oxidative stress. I found ROS levels (exposed to $H_2O_2$) were significantly decreased in TSA-MSCs compared with MSCs (Fig. 2A and 2B). I also have shown that TSA (0.1~5 μM) alone had not effect to ROS level in BM-MSCs (Fig. 3A and 3B).

Several reports have shown that the application of TSA at micromolar ranges inhibit cell growth, and cell death occurred due to increment of intracellular ROS [27, 31]. In this study, I have shown the TSA treatment at nanomolar ranges decreases ROS levels in oxidative stress induced hBM-MSCs (Fig. 2A and 2B). This inconsistency with our study may be caused by difference of TSA concentration. As shown figure 2B, treatment of TSA at high concentration did not affects the ROS production. These suggest that low molar concentration of TSA could be the protection from oxidative stress in hBM-MSCs.

Since TSA reduced the production of ROS, I examined the protective effects of TSA on oxidative damage in BM-MSCs. The cell viabilities from oxidative damage were improved in TSA-MSCs compared to ctrl-MSCs (Fig. 4). This result suggests that the treatment of TSA improves the protective capacities of stem cells against oxidative stress.

I described that TSA pretreatment to hBM-MSCs significantly reduces intracellular ROS. However, I do not confirm which genes are

directly involved in modulating intracellular ROS and which mechanisms act through any signaling pathway. Therefore, the relationship between TSA and intracellular ROS need to be further examined. It should be our next study.

In conclusion, I investigated protective effects of TSA on oxidative damage in BM-MSCs and confirmed the improvement of cell viability. This suggests that TSA treated MSCs prevent the cellular toxicities induced by oxidative stress. Therefore, optimized dose of TSA might be improved the stem cell potency and may provide better efficiency of stem cell therapy.

# V. References


[1] Pittenger, M.F., et al., Multilineage potential of adult human mesenchymal stem cells. Science, 1999. 284(5411): p. 143-7.

[2] Black, I.B. and D. Woodbury, Adult rat and human bone marrow stromal stem cells differentiate into neurons. Blood Cells Mol Dis, 2001. 27(3): p. 632-6.

[3] Nagai, A., et al., Multilineage potential of stable human mesenchymal stem cell line derived from fetal marrow. PLoS One, 2007. 2(12): p. e1272.

[4] Cho, G.W., et al., Bone marrow-derived stromal cells from amyotrophic lateral sclerosis patients have diminished stem cell capacity. Stem Cells Dev, 2010. 19(7): p. 1035-42.

[5] Sharpless, N.E. and R.A. DePinho, Telomeres, stem cells, senescence, and cancer. J Clin Invest, 2004. 113(2): p. 160-8.

[6] Rossi, D.J., et al., Deficiencies in DNA damage repair limit the function of haematopoietic stem cells with age. Nature, 2007. 447(7145): p. 725-9.

[7] Heeschen, C., et al., Profoundly reduced neovascularization capacity of bone marrow mononuclear cells derived from patients with chronic ischemic heart disease. Circulation, 2004. 109(13): p. 1615-22.

[8] Tepper, O.M., et al., Human endothelial progenitor cells from type II diabetics exhibit impaired proliferation, adhesion, and incorporation into vascular structures. Circulation, 2002. 106(22): p. 2781-6.

[9] Rota, M., et al., Diabetes promotes cardiac stem cell aging and heart failure, which are prevented by deletion of the p66shc gene. Circ Res, 2006. 99(1): p. 42-52.

[10] Geissler, S., et al., Functional comparison of chronological and in vitro aging: differential role of the cytoskeleton and mitochondria in mesenchymal stromal cells. PLoS One, 2012. 7(12): p. e52700.

[11] Song, H., et al., Reactive oxygen species inhibit adhesion of mesenchymal stem cells implanted into ischemic myocardium via interference of focal adhesion complex. Stem Cells, 2010. 28(3): p. 555-63.

[12] Chiarugi, P. and F. Buricchi, Protein tyrosine phosphorylation and reversible

oxidation: two cross-talking posttranslation modifications. Antioxid Redox Signal, 2007. 9(1): p. 1-24.

[13] Back, P., B.P. Braeckman, and F. Matthijssens, ROS in aging Caenorhabditis elegans: damage or signaling? Oxid Med Cell Longev, 2012. 2012: p. 608478.

[14] Bolden, J.E., M.J. Peart, and R.W. Johnstone, Anticancer activities of histone deacetylase inhibitors. Nat Rev Drug Discov, 2006. 5(9): p. 769-84.

[15] Minucci, S. and P.G. Pelicci, Histone deacetylase inhibitors and the promise of epigenetic (and more) treatments for cancer. Nat Rev Cancer, 2006. 6(1): p. 38-51.

[16] Machado-Vieira, R., L. Ibrahim, and C.A. Zarate, Jr., Histone deacetylases and mood disorders: epigenetic programming in gene-environment interactions. CNS Neurosci Ther, 2011. 17(6): p. 699-704.

[17]. Govindarajan, N., et al., Reducing HDAC6 ameliorates cognitive deficits in a mouse model for Alzheimer's disease. EMBO Mol Med, 2013. 5(1): p. 52-63.

[18]. Yildirim, F., et al., Inhibition of histone deacetylation protects wildtype but not gelsolin-deficient mice from ischemic brain injury. Exp Neurol, 2008. 210(2): p. 531-42.

[19] Koch-Weser, J. and T.R. Browne, Drug therapy: Valproic acid. N Engl J Med, 1980. 302(12): p. 661-6.

[20] Rogawski, M.A. and W. Loscher, The neurobiology of antiepileptic drugs. Nat Rev Neurosci, 2004. 5(7): p. 553-64.

[21] Drevets, W.C., Neuroimaging studies of mood disorders. Biol Psychiatry, 2000. 48(8): p. 813-29.

[22] Rajkowska, G., Postmortem studies in mood disorders indicate altered numbers of neurons and glial cells. Biol Psychiatry, 2000. 48(8): p. 766-77.

[23] Vanhaecke, T., et al., Trichostatin A-like hydroxamate histone deacetylase inhibitors as therapeutic agents: toxicological point of view. Curr Med Chem, 2004. 11(12): p. 1629-43.

[24] Yoo, Y.E. and C.P. Ko, Treatment with trichostatin A initiated after disease

onset delays disease progression and increases survival in a mouse model of amyotrophic lateral sclerosis. Exp Neurol, 2011. 231(1): p. 147-59.

[25] Wang, P., et al., Trichostatin A protects against cisplatin-induced ototoxicity by regulating expression of genes related to apoptosis and synaptic function. Neurotoxicology, 2013. 37: p. 51-62.

[26] Kang, J., et al., Nickel-induced histone hypoacetylation: the role of reactive oxygen species. Toxicol Sci, 2003. 74(2): p. 279-86.

[27] You, B.R. and W.H. Park, Trichostatin A induces apoptotic cell death of HeLa cells in a Bcl-2 and oxidative stress-dependent manner. Int J Oncol, 2013. 42(1): p. 359-66.

[28] Kujoth, G.C., et al., Mitochondrial DNA mutations, oxidative stress, and apoptosis in mammalian aging. Science, 2005. 309(5733): p. 481-4.

[29] Xuan, A., et al., Neuroprotective effects of valproic acid following transient global ischemia in rats. Life Sci, 2012. 90(11-12): p. 463-8.

[30] Agudelo, M., et al., Effects of alcohol on histone deacetylase 2 (HDAC2) and the neuroprotective role of trichostatin A (TSA). Alcohol Clin Exp Res, 2011. 35(8): p. 1550-6.

[31] Chou, C.W., et al., HDAC inhibition decreases the expression of EGFR in colorectal cancer cells. PLoS One, 2011. 6(3): p. e18087.

# VI. Acknowledgements

대학원에 입학한 것이 얼마 되지 않은 것 같은데 벌써 졸업 날이 다 되어 갑니다. 아직은 석사라는 이름을 받기에는 부족한 점이 많은데 부끄러울 뿐입니다. 지금까지 석사학위를 무사히 마칠 수 있도록 도와주신 분들께 감사의 인사를 드립니다. 먼저 저를 낳아주시고 길러주시고 세상에 두려움 없이 맞서도록 도와주신 아버지, 어머니 정말 감사 드립니다. 그리고 옆에서 항상 힘내라는 말과 함께 든든하게 지켜줬던 가족들 정말 감사합니다. 앞으로도 좀 더 저의 꿈을 향한 그리고 발전을 위한 길을 계속 가려 합니다. 끝까지 믿고 지켜봐 주세요.

그리고 저에 학위 생활을 앞장서서 지도해주시고 이끌어 주신 조광원 교수님 항상 감사 드립니다. 교수님의 첫 제자로서 부끄러움 없는 그리고 진취적인 학생이 되고자 항상 노력하겠습니다. 아직은 많이 부족한 학생이지만 앞으로 좀더 노력해서 부족한 부분들을 하나하나 채워가도록 하겠습니다. 그리고 저에 대학생활을 지켜봐 주시고 가르쳐 주시고 인도해주신 김영곤 교수님, 박현용 교수님께 감사의 말씀을 드리고 저에 학위 생활 동안 많은 가르침을 주신 전택중 교수님, 이준식 교수님께도 진심으로 감사의 말씀을 드립니다. 또한 제가 학과 학생은 아니지만 항상 아낌없는 조언과 지도를 해주신 온탁범 교수님 그리고 많은 도움을 주신 박라영 선생님께도 감사의 말씀을 드립니다. 저의 학위 과정 동안 항상 옆에서 함께 해왔던 우리 실험실 식구들, 윤서, 이슬이, 호태, 민지 항상 고맙게 생각한다는 마음을 이 자리에서 전합니다. 아울러 저와 대학생활부터 학위 생활까지 함께 해온 나의 동기 동환이, 실험적으로 다툼도 많이 있었지만 항상 함께 할 수 있어서 정말 든든했고, 동환이와 함께 저를 지지해주고 버팀목이 되어준 병호, 정선, 석희, 종배, 진태, 영희, 기수, 지일이에게 정말 고맙다는 말을 전하고 싶습니다.

그리고 힘들 때 고민을 들어주고 든든한 버팀목이 되어준 고등학교 친구들 길근이, 재우, 영표, 백진, 의연, 슬기, 그리고 지금은 함께 할 수 없지만 항상 곁에 있는 친구 세훈이에게 항상 고맙게 생각하고 있음을 전하고 싶습니다. 모든 소중한 분들이 있었기에 제가 지금 이 순간까지 버티며 전진해 나갈 수 있었습니다. 다시 한번 감사의 말씀을 드리며 또 다른 시작을 준비하는 만큼 여러분께 부끄럽지 않은 사람이 되도록 노력하겠습니다.